Eight-Membered-Ring Solid-State Conformational Interconversion via the Atom-Flip Mechanism, a CPMAS ^{13}C NMR and Crystallographic Stereochemical Study†

Robert Glaser,* Artem Novoselsky, and Dror Shiftan

Department of Chemistry, Ben-Gurion University of the Negev, Beer-Sheva 84105, Israel

Marc Drouin

Département de Chimie, Université de Sherbrooke, Québec, Canada J1K 2R1

glaser@bgumail.bgu.ac.il

Received February 2, 2000

Nefopam methohalide (chloride, bromide, and iodide) medium-ring quaternary ammonium salts of the non-narcotic analgesic tertiary amine drug give crystals belonging to the identical monoclinic $P2_1/c$ space group, and all of these pseudopolymorphs exhibit the same packing motif. A singular boat−boat (BB) more compact conformation is observed in the nefopam methochloride crystal. Larger halide anions (bromide and iodide) increase the void distance between the 2_1-screw axis related adjacent ammonium cations to accommodate void-size dependent equilibrium quantities of the twist-chair−chair (TCC) more extended conformation. The BB:TCC occupancy factors are 0.961(5):0.039-(5) [193 K], 0.780(5):0.220(5) [293 K], and 0.755(6):0.245(6) [343 K] for the methobromide crystal, while values of 0.657(5):0.343(5) [193 K] and 0.592(7):0.408(7) [293 K] were measured for the methiodide. Above a minimum of ca. 2.53 Å, the occupancy factors were found to be linearly correlated to the intermolecular (TCC)Me_{eq}−*H*···*H*−Me_{ax}(TCC) distance between abutting methyl group protons in 2_1-screw axis related neighbors. Temperature-dependent occupancy factors for the two conformers are interpreted in terms of a medium ring atom-flip facile interconversion between the two low energy conformations in crystals containing the appropriate size intercation void. A BB/TCC atom-flip interconversion in the methochloride unit cell would result in van der Waals interactions due to an estimated 2.31 Å close intermolecular (TCC)Me_{eq}−*H*···*H*−Me_{ax}(TCC) distance between adjacent 2_1-screw symmetry ammonium cations. The 203 K low-temperature CPMAS ^{13}C NMR spectrum of the methiodide salt showed two slow exchange limit (SEL) δ 57.91 [BB] and δ 63.10 [TCC] OCH_2CH_2N peaks. A variable low-temperature CPMAS NMR investigation of the solid methiodide showed complex dynamic behavior that cannot be interpreted solely on the basis of an atom-flip conformational interconversion. Local magnetic fields from the *gem*-dimethyl rapidly rotating proton magnetic dipoles provide a distance-dependent T_1 relaxation mechanism for neighboring carbons in the solid-state.

Introduction

Medium rings are generally considered to contain eight to twelve members.[1] Dale has extensively investigated the stereochemistry of medium size rings,[2] and has described seven conformations for cyclooctane. Strong torsional constraints limit the conformational possibilities for these rings, and only four were presented for *cis*-cyclooctene: boat−chair (BC), twist-chair−chair (TCC), boat−boat (BB), and twist-boat−chair (TBC).[3] Strong torsional constraints upon the conformations of medium-size rings can arise from a number of structural sources. We have recently reviewed the stereochemistry and interconversion of nine-membered rings containing one strong torsional constraint and have shown that double bonds, annelated three-membered rings (epoxides, aziridines, cyclopropanes, etc.), benzannelated rings, lactams, and sometimes lactones are among the many structural features used for this purpose.[4]

Nefopam hydrochloride [5-methyl-1-phenyl-3,4,5,6-tetrahydro-1*H*-2,5-benzoxazocine,[5] (**1**)] is a benzannelated eight-membered heterocyclic non-narcotic analgesic drug with antidepressant properties.[6] X-ray crystallographic determination of the structures of (+)-[7,8] and (−)[9] chiral crystals and of the racemic modification[7,8,10] of nefopam hydrochloride (**1**) showed the 2,5-benzoxazocine ring to

† This paper is dedicated to Prof. Harald Günther (Universität − Gesamthochschule Siegen, FRD) on the occasion of his 65th birthday.

(1) Sicher, J. *Prog. Stereochem.* **1962**, *3*, 202.

(2) Dale, J. *Stereochemistry and Conformational Analysis*; Universitetsforlaget/Verlag Chemie: Oslo/New York, 1978; p 197.

(3) Dale, J. *Top. Stereochem.* **1976**, *9*, 199.

(4) Glaser, R.; Shiftan, D. *Adv. Mol. Struct. Res.* **1999**, *5*, 89−151.

(5) *The Merck Index*, 12th ed.; Budavari, S., Ed.; Merck: Rahway, NJ, 1996; p 1105, and references therein.

(6) Klohs, M. W.; Draper, M. S.; Petracek, F. J.; Ginzel, K. H.; Ré, O. N. *Arzneim.-Forsch. (Drug Res.)* **1972**, *22*, 132.

(7) Glaser, R.; Cohen, S.; Donnell, D.; Agranat, I. *J. Pharm. Sci.* **1986**, *75*, 772.

(8) Glaser, R.; Frenking, G.; Loew, G. H.; Donnell, D.; Cohen, S.; Agranat, I. *J. Chem. Soc., Perkin Trans. 2* **1989**, 113.

(9) Hansen, L. K.; Hordvik, A.; Aasen, A. J. *Acta Chem. Scand.* **1984**, *38*, 327.

(10) Klüfers, P.; v. Petersenn, A.; Röder, E. *Arch. Pharm. (Weinheim)* **1986**, *319*, 583.

10.1021/jo000146g CCC: $19.00
Published on Web 09/13/2000

be bent into the boat-boat conformation (BB). This is illustrated in the 2D-iconic projection (**2**) of the actual 3D X-ray determined structure of (±)-**1**. Anet[11] has developed a general definition of axial, equatorial, and related descriptor terms for substituents on rings of any size. Using this general definition, the BB-**2** phenyl ring is located in a sterically free exo-oriented *pseudoequatorial* position, while the *N*-methyl group is located at a "corner position" and is nearly-isoclinal. A "corner" position in a ring was defined by Dale[12] as a ring-atom having two endocyclic bonds with identically signed gauche (synclinal, ca.60°) torsion angles (e.g., $+g,+g$ or $-g,-g$). He also noted that geminal substituents can only be accommodated in corner positions since neither of the groups are orientated toward the interior of the ring (i.e., they do not suffer from transannular interactions common to medium size rings).[13] In ideal C_2-symmetry medium rings, the rotation axis passes through a corner position, and the geminal substituents at these corners are exchanged by the rotation operation (i.e., they are homotopic by an internal comparison). They are isoclinal (equal "dip" or inclination, as noted by Hendrickson[14]) regarding their orientation vis-à-vis the ring; i.e., they cannot be assigned equatorial or axial ring-substituent descriptors. The stereolabile stereogenic and chirotopic nitrogen of tertiary ammonium salt BB-**2** resides at such a corner position.

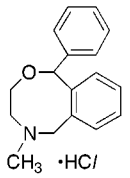

1

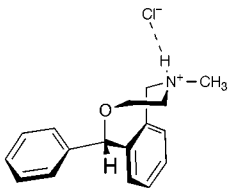

2

The ^{1}H NMR spectrum of crystalline **1** (BB-**2**) dissolved in CD_2Cl_2 or acidic aqueous medium showed two *N*-methyl diastereomers (**2** and **3** in a ca. 2:3 ratio, respectively), at the slow exchange limit (SEL) for interconversion.[7,15] These diastereomers resulted from epimerization at nitrogen via a prototropic shift/nitrogen inversion mechanism.[7,15] Relative orientations of the externally diastereotopic *N*-methyl groups were readily apparent from analysis of the ^3J(N*H*C*H*) vicinal coupling constants in the CD_2Cl_2 spectrum. Some of the multiplets showed line broadening, which sharpened upon a decrease in solvent temperature. Since no additional species were observed at low temperature, a putative "hidden partner" was deemed to be present at the fast exchange limit (FEL) for conformational interconversion. The vicinal coupling constants, and the O−C−C−N endocyclic torsion angle calculated using Lambert's[16] *R*-ratio of coupling constants, were all consistent with predominant BB conformations for each of the two *N*-methyl diastereomers.[7,15]

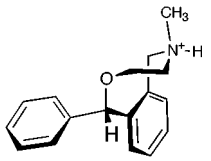

3

The ammonium nitrogen is no longer stereogenic in nefopam methohalide quaternary ammonium salts, and the two *N*-methyl groups therein are now internally diastereotopic. The ^{1}H and ^{13}C NMR spectra of these salts dissolved in CD_2Cl_2 also showed line-broadening for the single species.[17] Single-crystal X-ray crystallographic analysis of nefopam methiodide (**4**)[18] showed disorder between two conformational models (BB-**5** and TCC-**6**) which was found to be temperature dependent.[19] Upon refinement, the Fourier maps of disordered crystals, such as **4**, afford peaks of electron density corresponding to both models which are weighted by a refined parameter (the occupancy factor) that depends on the fraction of each model present in the crystal. A temperature dependence for these occupancy factors signifies that this disorder is "dynamic" in nature (rather than static). Dynamic disorders of this type testify to conformational interconversion within the confines of the crystal lattice. On the other hand, static disorder, e.g., (±)-*threo*-*N*-methylmethylphenidate HCl [*N*-methylritalin HCl],[20] is expected to exhibit temperature invariant occupancy factors which may differ according to the particular crystal under investigation.

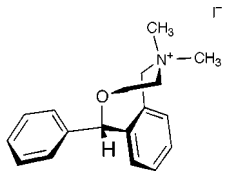

5

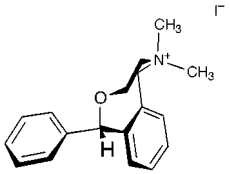

6

The greater mobility of medium-size rings permits conformational interconversions to take place in more localized step processes rather than as synchronous changes of the whole ring. These stepwise interconversion modes include atom-flips, bond torques, and endocyclic synperiplanar double-bond face-flips.[4] In this particular case, the *N*-methylene carbon of the O−CH_2−***C***H_2−N

(11) Anet, F. A. L. *Tetrahedron Lett.* **1990**, *31*, 2125−2126.
(12) Dale, J. *Acta Chem. Scand.* **1973**, *27*, 1115.
(13) Reference 2, p 206.
(14) Hendrickson, J. B. *J. Am. Chem. Soc.* **1964**, *86*, 4854.
(15) Glaser, R.; Frenking, G.; Loew, G. H.; Donnell, D.; Agranat, I. *New J. Chem.* **1988**, *12*, 953.
(16) Lambert, J. B. *J. Am. Chem. Soc.* **1967**, *89*, 1836.
(17) Glaser, R.; Peleg, A.; Geresh, S. *Magn. Reson. Chem.* **1990**, *28*, 389.
(18) Glaser, R.; Michel, A.; Drouin, M. *Can. J. Chem.* **1990**, *68*, 1128.
(19) Glaser, R.; Drouin, M. Unpublished results.
(20) Glaser. R.; Adin, I.; Shiftan, D.; Shi, Q.; Deutsch, H. M.; George, C.; Wu, K.-M.; Froimowitz, M. *J. Org. Chem.* **1998**, *63*, 1785.

fragment undergoes an "atom-flip" to the other side of the octagonal-ring mean plane and thereby interconverts the BB into the TCC conformation. This solid-state conformational interchange was the impetus for an X-ray crystallographic and CPMAS NMR investigation of a series of crystalline nefopam methohalide quaternary ammonium salts containing anions of increasing size (chloride, bromide, and iodide). The results of this study are reported below.

Results and Discussion

X-ray Crystallographic Studies of Nefopam Quaternary Ammonium Salts. The solid-state structures of nefopam methiodide (**4**) (193 and 293 K), nefopam methobromide (**7**) (193, 293, and 343 K),] and methochloride (**8**) (193 K) were determined at a number of temperatures by single-crystal X-ray diffraction analysis.[21] All the nefopam methohalides in this series gave crystals belonging to the identical monoclinic $P2_1/c$ space group, and all of them exhibited the same packing motif. The unit-cell volume (V) increased with increasing halide anion radius and crystal temperature. In the methochloride (**8**) (193 K), methobromide (**7**) (193, 293, 343 K), and methiodide (**4**) (193, 293 K) series, V increased from 1532.0, 1626.0, 1650.9, 1662.8, 1713.3, to 1742.1 Å^3, respectively. The a, b, and c lengths respectfully increased by 3.4, 2.2, and 1.6% from those of the low temperature (193 K) chloride small anion unit cell (**8**) to those of the ambient temperature (293 K) iodide large anion analogue (**4**), while intermediate increments were noted for **7** (193, 293, 343 K) and **4** (193 K). Numbering diagrams for the BB and TCC conformations of **7** are given as ball-and-stick structures **9** and **10**. The eight endocyclic torsion angles characterizing the BB conformation in the 193 K structure of **4** starting with C(11)−C(1)−O(2)−C(3) and continuing *clockwise* in **9** are −74.7(4), −14.0(2), 0.4(3), 84.1(4), −43.9(4), −59.9(4), 47.9(3), and 73.0(5) deg; while the corresponding angles in TCC-**10** are −74.7(4), −14.0(2), 0.4(3), 84.1(4), −89.6(7), 46.0(6), −59.9(7), and 122.0(8) deg, estimated standard deviation of last digit (esd's) given in parentheses.

Only the BB conformation was found for the methochloride, while a BB/TCC dynamic disorder was observed for the methobromide and methiodide. The BB:TCC occupancy factors were 0.961(5):0.039(5) (193 K), 0.780(5):0.220(5) (293 K), and 0.755(6):0.245(6) (343 K) for **7**; while values of 0.657(5):0.343(5) (193 K) and 0.592(7):0.408(7) (293 K) were measured for **4**. The set of six BB conformations are all the same as shown by superimposition[22] of the octagonal ring endocyclic atoms and N-methyl carbons in **8** (193 K), **7** (193, 293, 343 K), and **4** (293 K) upon corresponding atoms in **4** (193 K) to give very low root-mean-square (RMS) differences of only 0.056, 0.043, 0.037, 0.038, and 0.018 Å, respectively. Similarly, the series of five TCC conformations are also all the same as shown by a superimposition[22] of these same atoms in **7** (193, 293, 343 K), and **4** (293 K) upon corresponding atoms in **4** (193 K) to give root-mean-square (rms) differences of only 0.196, 0.054, 0.060, and 0.034 Å, respectively. The very low electron density for the 193 K TCC C(4B,13B,14B) atoms [0.039(5) TCC occupancy factor] is probably behind the relatively higher 0.196 Å rms value in the above comparison.

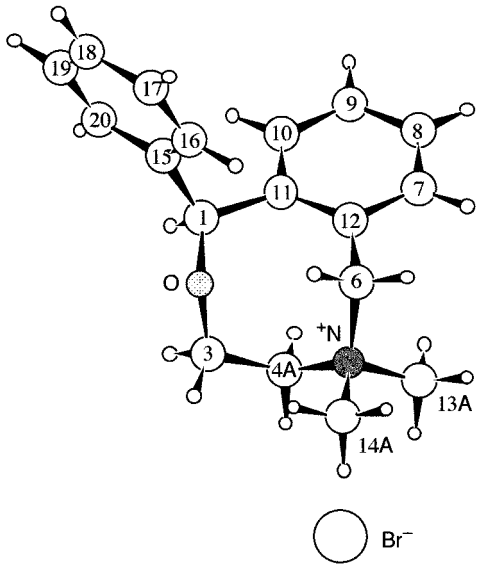

9

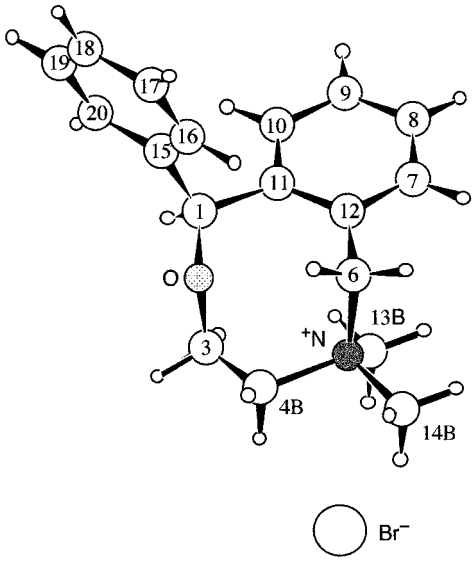

10

Inscription of a saturated eight-membered ring on a diamond lattice would result in a highly strained C_{2v} BB-conformation. The very severe transannular interactions between H(2-endo)···H(6-endo) and its S_4 symmetry related H(4-endo)···H(11-endo) atoms in such a BB-cyclooctane, would only be very marginally removed by subsequent twisting into a C_2 BB-conformation. However, placement of nonprotonated atoms at ring-positions 2 and 11 [O(2) and quaternary C(11)] enables these interactions to be either completely or partially removed in **9**. BB-**9** is more spatially "compact" compared to TCC-**10** and has been crystallographically found before for nefopam and N-desmethylnefopam salts.[7,8,23,24]

(21) The authors have deposited atomic coordinates for these structures with the Cambridge Crystallographic Data Centre. The coordinates can be obtained, on request, from the Director, Cambridge Crystallographic Data Centre, 12 Union Road, Cambridge, CB2 1EZ, U.K.

(22) Sundin, A. *MacMimic 3.0*; In−Star Software: Lund, Sweden, 1996.

(23) Glaser, R.; Geresh, S.; Blumenfeld, J.; Donnell, D.; Sugisaka, N.; Drouin, M.; Michel, A. *J. Pharm. Sci.* **1993**, *82*, 276.

(24) Glaser, R.; Blumenfeld, J.; Geresh, S.; Donnell, D.; Rosland, H.; Hole, K.; Maartmann-Moe, K. *J. Pharm. Sci.* **1992**, *82*, 886.

The TCC conformation was also been crystallographically observed for (1*RS*,3*RS*)-3-methylnefopam[24] HCl (**11**) and for **12**.[25] Although it appears that the H(4-endo)··· C(11) interaction in BB-**9** has been completely removed in the TCC-**10** analogue, ab initio[26] (RHF/6-31G* basis set) and density functional theory (DFT)[27] geometry optimized models of the secondary ammonium *N*-desmethylnefopam cation (in which the benzo ring has been replaced by a double bond) show that both conformations are practically the same in estimated energy. The BB conformation is more stable than TCC by only 0.28 kcal mol^{-1} for RHF/6-31G* models, while TCC is now more stable than BB by 0.27 kcal mol^{-1} for the B3LYP/6-31G-(d) density functional models. In solid-state packing, on the other hand, the TCC conformation has a higher degree of spatial extension. In crystalline **11**, the TCC arrangement is sterically favorable for the 3-methyl group due to its equatorial orientation relative to the C(3)−C(4)−N fragment. A BB conformation C(3)-methyl group would suffer a 1,3-cis-diaxial interaction with the axial proton ligated to the ammonium nitrogen. The equatorial *N*-methyl TCC preference for solid- and solution-state **12** (with its N−O moiety) is stereoelectronic in nature.[28] Only in this arrangement is the nitrogen lone pair removed as far away as possible from *each* of the adjacent oxygen lone-pairs (LP), i.e., two anticlinal (ca. 120°) LP−O−N−LP torsion angles [this strong stereoelectronic conformational constraint is also observed in the corresponding nine-membered ring analogue[4,29]].

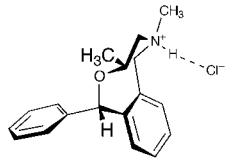

11

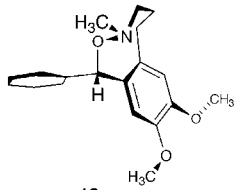

12

The nitrogen atom is no longer at a "corner" position in TCC-**10**, since the adjacent torsion angles are oppositely signed [e.g., 49.6(3)° C(3)−C(4B)−N−C(6) and −92.0(3)° C(4B)−N−C(6)−C(12) torsion angles for **7** at 293 K]. The *gem*-dimethyl groups can now be assigned conventional axial [C(13B)] and equatorial [C(14B)] descriptors according to Anet's[11] general method. The axial C(13B) methyl is oriented toward the octagonal ring interior. While the black colored H(3-ax,5-ax) protons in the saturated cyclooctane analogue **13** suffer transannular interactions with H(8-endo), this interaction [now with nonprotonated sp^2-C(11)] is considerably reduced in benzannelated **10**.

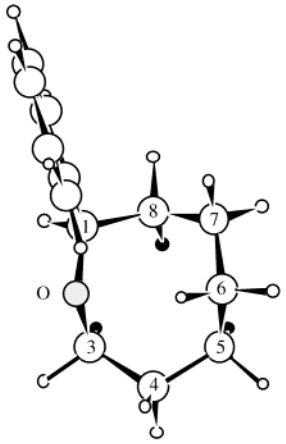

13

Although Anet's general method allows only nearly-isoclinal descriptors to be affixed to each of the *gem*-dimethyl carbons in BB-**9**, inspection of the structure shows that in relation to the C(3)−C(4)−N fragment we can assign relative equatorial and axial descriptors to C(13A) and C(14A), respectively. One methyl group in each conformation (BB/TCC) suffers a 1,3-cis-diaxial interaction with an H(3-ax) proton, while axial C(13B) in TCC-**10** is also spatially close to C(11). This transannular interaction is probably the reason both ab initio and density functional theory (DFT)[27] models show the TCC conformation to be slightly higher in energy than that for the BB: +1.55 kcal mol^{-1} (for RHF/6-31G* model)[26] and +1.71 kcal mol^{-1} (for B3LYP/6-31G(d) density functional model). The benzo ring has been replaced by a double bond in these geometry optimized models.

The interconversion of the two conformations proceeds by a facile C(4) atom-flip (see Figure 1). In this mechanism, the signs of the endocyclic synclinal torsion angles on either side of the flipping atom undergo sign reversal [e.g., for methiodide **4** at 193 K: +47.9(3)° O(2)−C(3)−C(4A)−N(5) and −59.9(4)° C(3)−C(4A)−N(5)−C(6) BB-torsion angles become −59.9(7)° O(2)−C(3)−C(4B)−N(5) and +46.0(6)° C(3)−C(4B)−N(5)−C(6) for the TCC conformer]. As a result of this ring-flip, *axial/equatorial* descriptors of six atoms are interchanged. Figure 1 shows that the axial H(3a,4a,),C(14) and equatorial H(3b,4b),C-(13) descriptors in BB−(**a**) interchange for corresponding atoms in TCC−(**b**). The temperature dependence of the occupancy factors for the methobromide and methiodide quaternary ammonium salts testify that this atom-flip occurs in the crystal lattice as well as in solution. A semiempirical AM1 torsion-angle driving study [constrained C(1)−O(2)−C(3)−C(4) and C(4)−N(5)−C(6)−C(12) endocyclic torsion angles] estimated the C(4) atom-flip transition-state to be 8.8 and 6.1 kcal/mol higher than the BB and TCC ground-states, respectively.

The unit-cell molecular contents of the three quaternary ammonium salts **4**, **7**, and **8** were calculated for each of the data sets measured at different temperatures in an attempt to gain insight into the singular conformation (BB) observed for the methochloride salt (**8**), and the higher TCC occupancy factor upon increase in halide anion radius and crystal temperature. The low degree of electron density for TCC C(4B,13B,14B) carbons in the 193 K dataset for **7** (vide supra), or the absence of the TCC conformer in the 193 K dataset for **8**, means that

(25) Bremner, J. B.; Browne, E. J.; Davies, P. E.; Raston, C. L.; White, A. H. *Aust. J. Chem.* **1980**, *33*, 1323.
(26) *MacSpartan Plus 1.2.1*; Wavefunction Inc.: Irvine, CA, 1999.
(27) *Gaussian-98W revision A-7*; Gaussian Inc.: Pittsburgh, 1998.
(28) Glaser, R.; Adin, I.; Drouin, M. Bremner, J. B. *New J. Chem.* **1995**, *19*, 1099.
(29) Bremner, J. B.; Browne, E. J.; Engelhardt, L. M.; Gunawardana, W. K.; White, A. H. *Aust. J. Chem.* **1988**, *41*, 293.

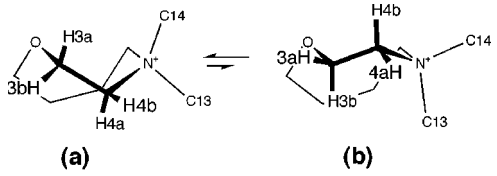

Figure 1. Interconversion of boat−boat (**a**) and twist-chair−chair (**b**) conformations via a C(4) atom flip in the eight-membered ring (phenyl and benzo rings have been removed for clarity).

193 K unit cells containing both BB/TCC conformations are either less exact (for **7**) or nonexistent (for **8**). In an identical arrangement to that crystallographically found for the methobromide (**7**) (293, 343 K) and methiodide (**4**) (193, 293 K) crystals, common atoms in the 193 K TCC conformation of **4** were superimposed on corresponding atoms in the BB 193 K datasets for **7** and **8** to give BB/TCC unit-cell models for the methobromide and methochloride datasets at the low temperature.

Dynamic motion of particular molecular subunits is well-known in the solid-state. For example, we have recently shown conformationally dependent differences in phenyl ring dynamic behavior by CPMAS NMR, despite the fact that the X-ray crystallographic anisotropic thermal parameters were similar for the phenyl-ring carbons.[30] Phenyl rings are immobile in compact conformation crystals of tertiary and quaternary scopolammonium[31] salts having ca. 2.5 Å close lateral neighbors on either face of the planar moiety.[30] However, these rings undergo a staccato-like rotation (called a "π-flip") in extended conformation crystals having ca. 3.0 Å close lateral neighbors on both faces of the aromatic plane.[30] Since inspection of the packing arrangements in these extended conformation crystals show that van der Waals H···H interactions prohibit phenyl ring free-rotation, this strongly suggests that lattice deformations enable the π-flip to be observed when the minimum space requirement is met. On the other hand, methyl groups readily rotate about their axes in the crystal state. For example, a typical methyl group at room-temperature jumps more than 10^9 times per second around its 3-fold axis,[32] and thus, X-ray crystallographers geometrically position hydrogens on methyl carbons. Structures **9** and **10** show a staggered arrangement for the *gem*-dimethyl hydrogens of both conformations.

Since the methohalides all crystallize in the same space group and pack in the same motif, it is likely that intermolecular close contacts are responsible for the varying degrees of TCC occupancy in the BB/TCC disordered salts **4** and **7**, and for the nonobservance of the more extended TCC conformation for **8**. There is a 2.92 Å minimum distance between equatorial methyl protons in one immobile BB conformation eight-membered ring, and axial methyl protons in the distant adjacent 2_1-screw symmetry related neighbor separated by a nearby upper chloride anion in the 193 K unit-cell as depicted in Figure 2 (methyl protons have been geometrically placed and subsequently isotropically refined). Protons in these two methyl groups are pushed away from each other as the anion size and crystal temperature increases. Portions

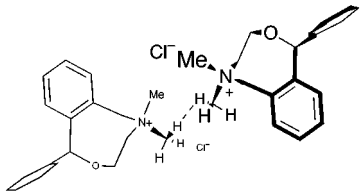

Figure 2. 3D-iconic projection of two 2_1-screw symmetry related BB neighbors in the 193 K methochloride unit-cell. The intermolecular distance between equatorial methyl protons in one molecule and axial methyl protons in the other are too close to each other to enable a C(4) atom flip.

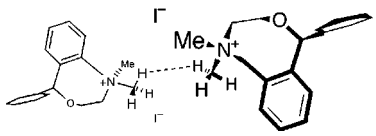

Figure 3. 3D-iconic projection of two 2_1-screw symmetry related TCC neighbors in a methiodide unit-cell. The intermolecular distance between equatorial methyl protons in one molecule and abutting axial methyl protons in the other have been correlated with the TCC occupancy factor.

of the *gem*-dimethyl substituted octagonal ring became mobile when this (BB)Me_{eq}−*H*···*H*−Me_{ax}(BB) minimum intermolecular distance increased to 3.17 Å in the methobromide 193 K unit-cell [0.961(5) BB occupancy factor]. When the distance further increased to 3.58 Å in the methiodide 193 K unit-cell, increased mobility was noted by the 0.657(5) lower BB occupancy factor value. Increasing intercation void size at constant 193 K temperature is clearly a function of anion size: e.g., $C(13A)_{BB}$···X^-···$C(14'A)_{BB}$ angles of 66° [X = chloride (**8**)], 69° [X = bromide (**7**)], and 74° [X = iodide (**4**)], where C(13) and C(14′) are the abutting equatorial and distant axial methyl carbons in adjacent 2_1-symmetry-related BB neighbors and X is the nearby upper halide anion illustrated in Figure 2. However, a linear relationship between the BB occupancy factor was not ascertained for either the (BB)Me_{eq}−*H*···*H*−Me_{ax}(BB) minimum intermolecular distance or for the $C(13A)_{BB}$···X^-···$C(14'A)_{BB}$ angle when datasets differing *both* in anion radius and crystal temperature were compared.

However, in those datasets where both anion radius and crystal temperature parameters differed, a good linear correlation was found between occupancy factors and the (TCC)Me_{eq}−*H*···*H*−Me_{ax}(TCC) minimum intermolecular distance between abutting geometrically placed and subsequently isotropically refined axial- and distant equatorial-methyl group protons in 2_1-screw axis related TCC-neighbors shown in Figure 3. TCC occupancy factors of 0.408(7) (MeI, 293 K), 0.343(5) (MeI, 193 K), 0.245(6) (MeBr, 343 K), 0.220(5) (MeBr, 293 K), and 0.039(5) (MeBr, 193 K) were correlated nicely with respective (TCC)Me_{eq}−*H*···*H*−Me_{ax}(TCC) intermolecular distances of 3.23, 3.13, 2.97, 2.90, and 2.59 Å to give the following linear relationship: $D_{Me-H\cdots H-Me} = (1.7491)(TCC_{occupancy\ factor}) + 2.525$, $\rho^2 = 0.998$. This correlationship predicts a zero TCC occupancy factor for (TCC)Me_{eq}−*H*···*H*−Me_{ax}-(TCC) minimum intermolecular distances ≤ 2.53 Å. The estimated ca. 2.31 Å (TCC)Me_{eq}−*H*···*H*−Me_{ax}(TCC) distance between adjacent molecules in our 193 K methochloride BB/superimposed-TCC unit-cell model is smaller than the zero TCC occupancy factor *y*-intercept value. Therefore, we can rationalize the crystallization of nefopam methochloride in an immobile more compact BB-

(30) Glaser, R.; Shiftan, D.; Drouin, M. *J. Org. Chem.* **1999**, *64*, 9217.
(31) Glaser, R.; Shiftan, D.; Drouin, M. *Can. J. Chem.* **2000**, *78*, 212.
(32) Schmidt-Rohr, K.; Spiess, H. W. *Multidimensional Solid-State NMR and Polymers*; Academic Press: London, 1994; p 174.

Table 1. Selected Solid-State CPMAS ^{13}C NMR Spectral Parameters for Nefopam Methohalide Quaternary Ammonium Salts (4, 7, and 8)[a]

	methiodide (**4**)		methobromide (**7**)	methochloride (**8**)		
atom	CPMAS	($CDCl_3$)[b]	CPMAS	CPMAS	T_1[c]	[min r(C···H−Me)]
C(1)	84.69	(86.39)	85.58	86.02	375	[4.26]
C(3)	66.15[d]	(65.24)	66.08[d]	66.50[e]	81	[2.70]
C(4)	62[f] vv brd	(58.37)	59.42[g] v brd	58.51[e]	29	[2.56]
C(6)	66.15[d]	(68.17)	66.08[d]	67.52[e]	37	[2.60]
C(7)	135.13	(135.08)[h]	135.18	136.71	111	[2.88]
C(8)		(128.54)		129.16	203	[3.81]
C(9)		(131.15)		130.3(4)[i]	≥271[j]	[4.50]
C(11)[k]	145.07	(143.43)	145.36	146.47[l]	241	[3.71]
C(12)[k]	123.44	(124.27)	123.52	123.71[l]	138	[2.80]
C(13)	53.82 brd	(53.09)	52.50 brd	52.73[l]	0.1	[−]
C(14)	49.62 brd	(50.86)[m]	50.31 brd	49.94[l]	0.1	[−]
C(15)[k]	142.68	(140.76)[n]	143.16	143.46[l]	323	[5.12]

[a] Ppm, 125.76 MHz, external spectral reference: glycine δC(=O) 176.03, VACP {TPPM-^{1}H}, spin-rate 12.75 kHz, 294.5 and 312 K probehead and internal rotor temperatures, respectively. [b] $CDCl_3$ solution-state δ values for **4** in parentheses, internal spectral reference: tetramethylsilane (TMS), protonated carbon assignments by $^{13}C/^1H$ 2D-HMQC, other solution-state δC_{Ar}: 129.29 C(10), 127.64 C(16,20), 128.89 C(17,19), 128.66 C(18); δH_{Ar} ($CDCl_3$) values for **4** are: 7.60 H(7) [dd, 1H, 1.6, 7.3 Hz], 7.41 H(8) [dt, 1H, 1.5, 2 × 7.5 Hz], 7.45 H(9) [dt, 1H, 1.7, 2 × 7.5 Hz], 7.20 H(10) [dd, 1H, 1.2, 7.4 Hz], 7.11 H(16,20) [dd, 2H, 1.8, 7.8 Hz], and 7.30−7.74 H(17−19) [m, 3H]. [c] T_1 values (s), carbon distance (Å) to closest methyl proton given in square brackets. [d] Unresolved broadened peak. [e] Sole peaks in negatively phased "methylene-only" CPPI spectrum. [f] Very very low intensity broad hump. [g] Low intensity very broadened peak. [h] Irradiation of HMQC correlated H(7) affords a 4.1% NOE intensity enhancement to δ 4.80 H(6-exo). [i] Mean δ value for 130.66, 130.29, and 129.93 δ (3C, 271 s T_1) close peaks which are not resolved in the T_1 experiment; estimated standard deviation of last digit is given in parentheses; assignment based upon T_1 value. [j] Other unassigned δC_{Ar} for solid **8**: 128.39 (1C, 333 s T_1); and 127.44, 127.23, 127.03 δ (3C, 298 s T_1). [k] Assignment based on GIAO δC_{calcd} values calculated from a BB-conformation DFT/B3LYP model. [l] $C_{quat.}$ or C_{methyl} observed in 60 μs dipolar dephasing delay NQS spectrum. [m] Irradiation of HMQC correlated δ 3.78 axial-H(methyl) affords a 2.3% NOE intensity enhancement to H(3-axial). [n] Assignment based upon $^{13}C/^1H$(long-range) 2D-HMBC.

conformation due to lack of sufficient void space to accommodate BB/TCC conformational interconversions. As the ca. 2.53 Å minimum distance increases, the intercation void becomes larger than the sum of the abutting van der Waals hydrogen-radii, and a C(4) atom-flip now enables the BB to interconvert into the more extended TCC conformation, since both are relatively low energy forms. Thus, one can now rationalize the decreasing methochloride ≫ methobromide > methiodide BB/TCC barriers in the set of methohalide lattices.

Solid-State CPMAS ^{13}C NMR Spectroscopy of Nefopam Quaternary Ammonium Salts. All resonances in the solution-state ^1H and $^{13}C\{^1H\}$ NMR ($CDCl_3$) spectra of **4** have now been assigned (with the use of $^1H/^1H$ NOE, DEPT-135, DEPT-90, and 2D-HMQC techniques) since this is important for subsequent assignment of CPMAS ^{13}C resonances. ^{13}C ($CDCl_3$) aromatic chemical shifts are presented in Table 1.

The BB/TCC equatorial protons in Figure 1 are all trans (antiperiplanar, ca. 180°) to electronegative atoms (oxygen and nitrogen), and thus one expects very small magnitude values (ca. 1.0−1.5 Hz) for the synclinal dihedral angle $^3J_{eq-eq'}$ vicinal coupling constant for each conformation.[34] Similarly, an antiperiplanar dihedral arrangement between BB/TCC axial protons would give rise to large ca. 11−12 Hz magnitude values for $^3J_{ax-ax'}$. Conformational equilibria containing appreciable quantities of both BB and TCC conformations at the FEL would afford weighted time-averaged values since diaxial H(3a,-4a) nuclei in Figure 1 BB-(**a**) now become diequatorial in TCC-(**b**) [while diaxial H(3b,4b) nuclei in TCC-(**b**) become diequatorial in BB-(**a**)]. The observation of extreme magnitude 12.8 Hz ($^3J_{ax-ax'}$), and <1 Hz ($^3J_{eq-eq'}$) values [together with 4.3 Hz ($^3J_{ax-eq'}$), and 3.8 Hz ($^3J_{eq-ax'}$)] reported[17] for the methiodide salt in CD_2Cl_2 solution (similar values in $CDCl_3$) clearly testify to a very strong conformational bias in this medium. Since line-broadening of ^1H and ^{13}C NMR resonances is also clearly evident, this dynamic behavior points to a very minor quantity of a second conformational species (i.e., a "hidden partner").[17,34] Unfortunately, the finding of 50.6(3)° BB-**6** and −59.3(3)° TCC-**6** (293 K) similar magnitude synclinal torsion angles for the O−C(3)−C(4)−N fragment does not permit us to ascertain which conformation predominates in solution. Solid-state conformational polymorphism (or pseudopolymorphism, in the case of quaternary ammonium salts **4**, **7**, and **8**) provides an opportunity to resolve this question. While flexible molecules usually exhibit weighted time-averaged structures in solution, the confines of the crystal lattice entrap one of the low energy structures and thus enable its CPMAS NMR spectral characterization. This approach was recently used to ascertain the different conformational preferences of the anticholinergic drug scopolamine hydrobromide in CD_2Cl_2 and in aqueous medium.[30] Only sharp lines for one single species were observed in the CPMAS spectrum for the methochloride (**8**), which was found to exist solely in the BB conformation by X-ray crystallography. Table 1 shows that the series of aliphatic ^{13}C chemical shift values for solid-state BB-**8** compare very closely with those measured for the quaternary ammonium salt in $CDCl_3$ solution (rms difference of only 0.7 ppm between the sets of six values). This strongly suggests that the predominant $CDCl_3$ solution-state conformation is also BB.

Dynamic NMR is readily apparent upon examination of the room-temperature ^{13}C CPMAS NMR spectra of nefopam methohalides **4** and **7** compared to **8** (see Figure 4). The solid-state chemical shifts for these salts are listed in Table 1. Three solid-state spectral editing experiments were used for assignments. The cross-polarization/polarization inversion[33] (CPPI) technique provides a "methylene-only" spectrum, in which the sole signals

(33) Wu, X.; Zilm, K. W. *J. Magn. Reson.* **1993**, *A102*, 205 and *ibid.* **1993**, *A104*, 119.
(34) Glaser, R. *Magn. Reson. Chem.* **1989**, *27*, 1142.

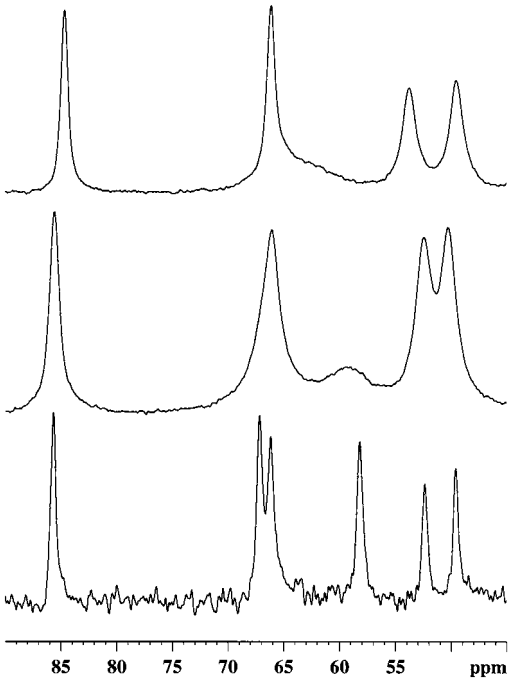

Figure 4. Comparison of expanded aliphatic spectral regions in isothermal (294.5 K probehead temperature, 312 K internal rotor temperature) CPMAS ^{13}C NMR (VACPTPPM, 12.75 kHz spin-rate) spectra showing dynamic C(4) broadening as a function of increasing anion size in crystalline $P2_1/c$ space group nefopam methohalide salts **4**, **7**, and **8** and concomitant increase in TCC occupancy within the BB/TCC C(4) atom-flip dynamic equilibrium. Lower trace: sharp δ 58.51 C(4) resonance for nefopam methochloride (**8**) with BB occupancy factor of 1.00; middle trace: broadened δ 59.42 C(4) for nefopam methobromide (**7**) with 0.780(5):0.220(5) BB:TCC occupancy factor ratio; upper trace: very broadened δ ca. 62 C(4) for nefopam methiodide (**4**) with 0.592(7):0.408(7) BB:TCC occupancy factor ratio (X-ray crystallographically determined occupancy factors, 293 K).

were negatively phased C(3,4,6) resonances; 50 μs dipolar-dephasing delay (NQS) spectra affords signals from nuclei having inefficient T_2 dipolar relaxation [i.e., C(13,-14) methyl and C(11,12,15) quaternary carbons]; while fast inversion recovery (a single 20 s T_1 delay) removes signals from methyl carbons.

The major difference between the CPMAS ^{13}C NMR spectra of the three quaternary ammonium salts (**4**, **7**, **8**) is in the appearance of the C(4) resonances, and the loss of C(3,6) signal resolution for the dynamic methohalides **4** and **7** (see Figure 4). The 58.5 ppm CPPI C(4A) resonance for the methochloride sole BB-conformation was sharp [66 Hz width at half-height ($W_{1/2}$)] and was assigned on the basis of finding a corresponding 58.4[34] ppm value for C(4) in $CDCl_3$ solution [assigned by 2D-HMQC NMR correlation to H(4-ax,eq)]. However, C(4) nuclei exhibit considerable line broadening in CPMAS spectra of the conformationally dynamic solid methobromide (**7**) and methiodide (**4**). $W_{1/2} = 490$ Hz for the δ 59.4 C(4) in **7**, while that for **4** is an even-lower intensity broad-hump at ca. 62 ppm. For comparison, $W_{1/2}$ is 106 Hz for C(1) in **7**, while it is only 54 Hz in the immobile BB-methochloride **8**.

Variable low-temperature CPMAS ^{13}C NMR experiments were untaken to probe the dynamic phenomenon exhibited in the ambient temperature spectra of **4** and **7**. The crystalline methiodide (**4**) was chosen since X-ray crystallography showed the TCC minor conformation to still be present with a fairly large 0.343(5) occupancy factor in the low temperature (193 K) single crystal. The TCC occupancy factor is only 0.039(5) for methobromide (**7**) at this temperature. At 203 K, four signals (δ 66.50, 63.11, 57.98, and 51.95) were observed in the range of 70−48 ppm, and their area ratios were respectively 2.00: 0.16:0.75:2.09. The C(3A,B) and C(6A,B) signals were not resolved at this lower temperature. The SEL δ 57.98 [C(4A) BB] and δ 63.11 [C(4B) TCC] two externally diastereotopic peaks at 203 K had a normalized peak area ratio of 0.82:0.18, respectively [X-ray crystallographically determined BB:TCC occupancy factor ratio of 0.657(5): 0.343(5) at 193 K]. However, only a *single* resonance (δ 51.95) was observed for the four diastereotopic methyl carbons [C(13A,B) and C(14A,B)]. Moreover, while the C(4A,B) peaks underwent coalescence at 273(2) K upon increasing temperature, the single methyl signal increasingly broadened under these same conditions and then became a "broad tabletop" at 273 K, and finally in the 278 K spectrum afforded δ 53.4 and 49.9 broadened methyl signals which continued to narrow upon further temperature increase. Although a C(4A,B) atom-flip conformational interchange readily explains the dynamic disorder on the X-ray crystallographic time-scale, clearly the dynamic phenomenon is more complex on the CPMAS NMR time-scale. It is well-known that these two time-scales can differ, e.g., X-ray crystallographically determined phenyl carbon atom anisothermal parameters are very similar for (−)-scopolamine hydrobromide anhydrate (extended conformation) and sesquihydrate (compact conformation) pseudopolymorph crystals, although their CPMAS NMR spectra readily shows a phenyl dynamic "π-flip" in the anhydrate while the ring remains immobile in the sesquihydrate.[30]

In the 203 K SEL CPMAS spectrum for **4**, BB δC(4A) exhibits a γ-*gauche* effect which characteristically shifts its value 5.2 ppm closer to TMS relative to that for the TCC conformer. This is rationalized by a *endo*-H(4-axial)···C(12) *cis*-1,3-diaxial-type interaction in **9** [i.e., an average 45(1)° C(4)−N−C(6)−C(12) torsion angle for the six BB structures in this study versus an *orthogonal* magnitude −91(3)° value for the same parameter in the five TCC analogues]. The CPMAS 122.4, 123.7, and 123.4 ppm values for C(12) in crystalline (±)-**1**, **8**, and (1*RS*,3*SR*)-3-methylnefopam[24] (**14**) also appear to result from this BB-conformation γ-gauche effect since C(12) is within the 127−129 ppm envelope for the TCC crystalline (1*RS*,3*RS*)-3-methylnefopam[24] epimer **11**.

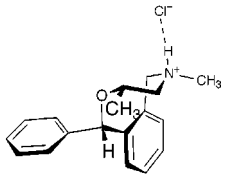

14

In a recent study involving 9- and 10-membered medium ring compounds; Grant and co-workers have provided insight into the nature of the γ-gauche effect involving methyl groups.[35] Repulsive steric interactions between methyl protons and proximate neighboring

(35) Harper, J. K.; McGeorge, G.; Grant, D. M. *J. Am. Chem. Soc.* **1999**, *121*, 6488.

protons correlated with large upfield shifts (lower frequencies) in two of the three methyl carbon tensor principle components.[35]

Finally, in addition to the single 20 s T_1 delay fast inversion recovery "spectral editing" experiment to remove methyl carbon signals noted above, an extensive study was also undertaken to specifically determine T_1 values of ^{13}C nuclei in the methochloride salt (**8**). The rotatable *N*-methyl carbons[32] [C(13A,14A)] exhibit characteristically very short T_1 values of only ca. 0.1 s (as opposed to much longer solid-state values typical for carbons ligated to immobile protons). Within a series of carbon nuclei having similar proton multiplicity (e.g., the three aromatic quaternary carbons, etc.), T_1 values were observed to dramatically shorten as the ^{13}C nucleus location became closer to protons in the *gem*-dimethylammonium moiety of the BB-molecule. For example, C(4A) and C(6) nuclei are both located ca. 2.6 Å away from the closest proton in each of the two methyl groups and exhibit $T_1 = 29$ and 37 s, respectively, while T_1 for the farther C(3) is 81 s in accord with ca. 2.7 and 4.0 Å distances from the closest proton in each methyl group. The three aromatic quaternary carbons C(12,11,15) show marked T_1 differences of 138, 241, and 323 s in accord with ca. 2.8, 3.7, and 5.1 Å distances from the nearest methyl group proton, respectively. Only the solution-state δ 140.76 C(15) resonance (and corresponding CPMAS δ 143.5 value) could be equivocally assigned by 2D-HMBC long-range correlation. However, these quaternary nuclei can indeed be assigned since $\delta^{13}C_{calcd}$ values of 123.4 C(12), 144.5 C(11), and 137.0 C(15) calculated from scaled GIAO isotropic magnetic shielding tensors (σ_{calcd}) correlate with the respective $\delta^{13}C_{exptl}$ 123.7, 146.5, and 143.5 CPMAS values. Finally, benzo-ring aromatic methine C(7,8,9) carbons afford T_1 values of 111, 203, and $\geq$271 s consistent with ca. 2.9, 3.8, and 4.5 Å distances from the nearest methyl group proton. These findings strongly suggest that local magnetic fields from the two sets of rapidly rotating methyl proton magnetic dipoles provide a distance-dependent relaxation mechanism for neighboring carbons in the solid-state.

Conclusion

In conclusion, this study provides insight into the singular BB more compact conformation observed in the nefopam methochloride crystal. Larger halide-anions (bromide and iodide) increase the void distance between 2_1-screw axis related adjacent ammonium cations to accommodate void-size dependent equilibrium quantities of the TCC *more extended* conformation. Temperature-dependent occupancy factors for the two conformers, and the broadened δ 59.4 C(4) signal in the methobromide ^{13}C CPMAS NMR spectrum, are interpreted in terms of a medium ring atom-flip facile interconversion between the two low energy conformations in crystals containing the appropriate size intercation void.

Experimental Section

(±)-Nefopam methohalides [iodide (**4**), bromide (**7**), and chloride (**8**)] were prepared by reaction of a methanolic solution of nefopam free base with an excess of the corresponding methyl halide at ambient temperature, under stirring, followed by in vacuo evaporation to dryness. Nefopam hydrochloride was a gift of Mr. David Donnell (3M Pharmaceuticals, Inc.).

Crystallography. Crystallization was performed by vapor diffusion of acetone into an absolute ethanolic solution of **4**, **7**, or **8** to yield clear colorless, crystalline prisms, belonging to the monoclinic system $P2_1/c$; mp 253−256°C dec (**4**), 276−280°C dec (**7**), and 273−275°C dec (**8**) °C. Crystal **7** was ground into a spherical shape. Table 2 provides crystallographic and data collection details for **4**, **7**, and **8**. The NRCVAX programs[36] were used for centering, indexing, and data collection. Data crystals were chosen having approximate dimensions of 0.20 × 0.30 × 0.30 (**4**), 0.50 × 0.50 × 0.50 (**7**), and 0.40 × 0.40 × 0.15 mm^3 (**8**). Crystallographic measurements were made on an Enraf-Nonius CAD-4 automatic diffractometer with graphite-monochromated Mo Kα_1 ($\lambda = 0.70930$ Å) radiation. The unit cell dimensions were obtained by a least-squares fit of 24 carefully centered reflections in the range of $30.0° \leq 2\theta \leq 40.0°$. Data were collected using the $\omega/2\theta$ scan technique to a maximum 2θ value of 50.0° with the exception of 44.8° and 49.8° for **4** at 193 and 293 K, respectively. Scans were made with a scan speed of 4 deg min^{-1} and a background time/scan time ratio of 0.25. During data collection, the intensities of two standard reflections were monitored every 60 min. No significant decay was observed.

The structures were solved by the application of direct methods and refined by least squares using the NRCVAX program.[36] An isotropic extinction coefficient was included in the refinement[37] to account for secondary extinction effects;[38] its values are given in Table 2. Empirical absorption corrections were made since the minimum and maximum transmission factors were 0.663 and 0.665 for the methiodide crystal, 0.536 and 0.543 for the methobromide crystal, as well as 0.999 and 0.950 for the methochloride crystal. Atomic scattering factors stored in the NRCVAX program were those of Cromer and Waber.[39] All non-hydrogen atoms in structures were refined anisotropically. Nonmethyl hydrogens for **8** were found in the difference Fourier map, and were refined isotropically. Hydrogens for **4**, **7** and methyl hydrogens for **8** were placed at their calculated positions, and were refined isotropically. The $R(F)$ and $R_w(F)$ final discrepancy indices at convergence for the $I_{net} \geq 2.5\sigma(I_{net})$ significant reflections refined with 218 parameters, 0 restraints, and 0 constraints [with the exception of 36 constraints for **7** (193 and 293 K)], as well as the GoF are listed in Table 2.

Molecular Modeling and Graphics. Restricted Hartree−Fock ab initio geometry optimizations using a 6-31G* basis set were performed using the MacSpartan Plus 1.2.1[26] program. Gauge independent atomic orbital (GIAO) RHF/6-311+G(2d,p) calculations [NMR keyword] based upon density functional theory B3LYP/6-31G(d) geometry optimized models were performed with the Gaussian-98W revision A-7[31] program. Based upon experimentally determined ^{13}C chemical shifts for rigid molecules, a scaling factor for the GIAO isotropic magnetic shielding tensors (σ_{calcd}) determined by the above protocol was found: $\delta_{expt}{}^{13}C = -0.88145 \cdot \sigma_{calcd}{}^{13}C + 179.14$ ($\rho^2 = 0.993$, 3.7 ppm rms difference between δ_{calcd} and δ_{expt} for $n = 26$ ^{13}C values. Noniconic molecular graphics **9**,**10** and **13** were drawn with the Ball&Stick[40] program. 2D-iconic projections of the X-ray crystallographic 3D-structures (**2**, **5**, **6**, **11**, **12**, **14** and Figures 1−3) or molecular models (**3**) were generated using the combination of *CS-Chem3D Pro 5.0* and *CS-ChemDraw Ultra 5.0* programs.[41] Superimposition of molecular structures were performed with the MacMimic 3.0 program.[22]

(36) Gabe, E. J.; Lee, F. L.; LePage, Y. The NRCVAX Crystal Structure System in Crystallographic Computing, In *Data Collection, Structure Determination, Proteins, and Data Bases*; Sheldrick, G. M., Kruger, C., Goddard, R., Eds.; Clarendon Press: Oxford, 1985; Vol. 3, pp 167−174.

(37) Larson, A. C. *Acta Crystallogr.* **1967**, *23*, 664.

(38) Zachariasen, W. H. *Acta Crystallogr.* **1963**, *16*, 1139.

(39) Cromer, D. T.; Waber, J. T. In *International Tables for X-ray Crystallography*; Ibers, J. A., Hamilton, W. C., Eds., Kynoch Press: Birmingham, 1974; Vol. IV, pp 99−101, Table 2.2B. (Present distributor Kluwer Academic Publishers: Dordrecht).

(40) Müller, N. *Ball&Stick 3.8*; Johannes Kepler University: Linz, 1999.

Table 2. Crystallographic Details for (±)-Nefopam Methiodide (4), (±)-Nefopam Methobromide (7), and (±)-Nefopam Methochloride (8)

	4	**7**	**8**	**4**	**7**	**7**
formula	$C_{18}H_{22}INO$	$C_{18}H_{22}BrNO$	$C_{18}H_{22}ClNO$	$C_{18}H_{22}INO$	$C_{18}H_{22}BrNO$	$C_{18}H_{22}BrNO$
FW, amu	395.29	348.28	303.83	395.29	348.28	348.28
space group	$P2_1/c$	$P2_1/c$	$P2_1/c$	$P2_1/c$	$P2_1/c$	$P2_1/c$
a, Å	9.951(1)	9.675(5)	9.523(1)	10.001(1)	9.7283(5)	9.7508(8)
b, Å	9.848(2)	9.712(4)	9.654(1)	9.928(1)	9.7531(5)	9.7848(5)
c, Å	17.539(2)	17.322(7)	17.208(2)	17.598(1)	17.415(1)	17.443(1)
β, deg	94.570(8)	92.37(4)	90.52(1)	94.41(1)	92.395(5)	92.371(6)
V, Å^3	1713.3(4)	1626(1)	1582.0(4)	1742.1(3)	1650.9(2)	1662.8(2)
Z	4	4	4	4	4	4
ρ_{calc}, g cm^{-3}	1.532	1.423	1.276	1.507	1.401	1.391
T, K	193	193	193	293	293	343
linear abs. coeff., mm^{-1}	1.85	2.53	0.24	1.84	2.46	2.44
collection range	$\pm h, +k, +l$ $-10 \le h \le 10$ $0 \le k \le 10$ $0 \le l \le 18$	$\pm h, +k, +l$ $-11 \le h \le 11$ $0 \le k \le 11$ $0 \le l \le 20$	$\pm h, \pm k, \pm l$ $-11 \le h \le 11$ $-11 \le k \le 11$ $-20 \le l \le 20$	$\pm h, +k, +l$ $-10 \le h \le 11$ $0 \le k \le 11$ $0 \le l \le 20$	$\pm h, +k, +l$ $-11 \le h \le 11$ $0 \le k \le 11$ $0 \le l \le 20$	$\pm h, +k, +l$ $-11 \le h \le 11$ $0 \le k \le 11$ $0 \le l \le 20$
isotropic extinction coeff., μm	0.12(1)	0.15(6)	0.016(1)	0.08(1)	0.15(6)	0.27(11)
total data/R_{merge}	6463/0.015	8176/0.011	10725/0.025	5949/0.014	8028/0.012	8495/0.010
unique data	2232	2863	2788	3388	2926	2920
unique data [$I_{net} \ge 2.5\sigma(I_{net})$]	1925	2299	2187	2765	2074	2078
max shift/σ	0.042	0.05	0.07	0.035	0.001	0.08
weighting factor, *w*	$(\sigma F_{obs}^2)^{-1}$	$(\sigma F_{obs}^2 + 0.0005F_{obs}^2)^{-1}$	$(\sigma F_{obs}^2 + 0.00005F_{obs}^2)^{-1}$	$(\sigma F_{obs}^2 + 0.0001F_{obs}^2)^{-1}$	$(\sigma F_{obs}^2 + 0.0005F_{obs}^2)^{-1}$	$(\sigma F_{obs}^2 + 0.00075F_{obs}^2)^{-1}$
$R(F)$[a] [$I_{net} \ge 2.5\sigma(I_{net})$]	0.033	0.039	0.032	0.037	0.041	0.042
$R_w(F)$[b] [$I_{net} \ge 2.5\sigma(I_{net})$]	0.040	0.050	0.031	0.038	0.053	0.055
goodness of fit[c]	1.75	1.72	1.90	1.74	1.80	1.51
largest diff. peak, e·Å^{-3}	+1.01	+0.80	+0.22	+1.02	+0.63	+0.62
largest diff. hole, e·Å^{-3}	−1.23	−0.75	−0.19	−0.98	−0.59	−0.37

[a] The final discrepancy index $R(F) = (\Sigma_i||F_{obs}|_i - |F_{calc}|_i)/(\Sigma_i|F_{obs}|_i)$. [b] The weighted value $R_w(F) = \mathrm{SQRT}[(\Sigma_i\{w_i(|F_{obs}|_i - |F_{calc}|_i)\}^2)/(\Sigma_i\{w_i(|F_{obs}|_i)\}^2)]$, where the particular weighting factor w_i is given in the table. [c] Goodness of fit = SQRT[$(\Sigma_i\{w_i(|F_{obs}|_i - |F_{calc}|_i)\}^2)$/(no. of reflections − no. of parameters)].

NMR Spectroscopy. Solid-state CPMAS ^{13}C NMR spectra were recorded at 125.76 MHz at 294.5 K on a Bruker DMX-500 FT NMR spectrometer equipped with a BL-4 CPMAS probehead and a High Resolution/High Performance (HPHP) ^{1}H preamplifier for solids. Spectra were calibrated with an external spectral reference (for solids, glycine δcarbonyl = 176.03) or an internal spectra reference (tetramethylsilane for $CDCl_3$). A VACPTPPM (variable amplitude cross-polarization/two pulse phase modulation ^{1}H decoupling) pulse-program was used for CPMAS spectra. NQS (nonquaternary and nonmethyl signal suppression, 50 μs T_2 dipolar dephasing delay period) and CPPI[33] (cross-polarization/polarization inversion) pulse-programs were utilized to afford spectral-editing giving "quaternary-/methyl-only" and "methylene-only" spectra, respectively. The fast inversion−recovery (FIR) technique was used to measure T_1 of carbon nuclei. Samples were placed in 4 mm zirconia rotors, and spun at a rate of 12.75 kHz for all spectra (with the exception 5.0 kHz for CPPI, and 6.0 kHz for CPTPPM variable temperature). Using the lead nitrate thermometer technique,[42] at 5.0, 6.0, and 12.75 kHz spin-rate the internal rotor temperature is respectively −0.8, +0.5, and +17.5 K relative to that in a nonspinning rotor at 294.5 K.[31]

Acknowledgment. Thanks are extended to Mr. David Donnell (3M Pharmaceuticals Inc.) for the gift of nefopam hydrochloride. The assistance of Dr. Yaacov Vinik (Kofolk Chemicals Ltd.) in the preparation of nefopam methochloride and methobromide is gratefully acknowledged. Gratitude is also expressed to Prof. Gernot Frenking and Dr. Martin Stahl (Philipps Universität, Marburg, FRD) for IGLO-II type preliminary calculations. The Bruker DMX-500 spectrometer and related equipment at The University Laboratory for Magnetic Resonance (Ben-Gurion University of the Negev) were purchased with matching funds grants from the Israel Ministry of Science and Industry, while the solid-state CPMAS accessory and HPHP solids ^{1}H preamplifier were purchased with matching funds grants from the Israel Academy of Sciences and Humanities Equipment Program and the Center for Natural Polysaccharides (BGU).

Supporting Information Available: Tables 3−17 for fractional coordinates for non-hydrogen and hydrogen atoms, interatomic bond distances, bond angles, torsion angles, and anisotropic thermal parameters for **4**, **7**, and **8**, Figure 5 [CPMAS ^{13}C NMR (VACPTPPM, 12.75 kHz spin-rate, 312 K internal rotor temperature) spectra for **4**,**7**, and **8**], Figure 6 [CPMAS ^{13}C NMR (CPTPPM, 6.0 kHz spin-rate, 203 K) spectrum for **4**], and Figure 7 [stack plot of 70−48 ppm region of the 203−286 K variable temperature CPMAS ^{13}C NMR (CPTPPM, 6.0 kHz spin-rate) spectra for **4**]. This material is available free of charge via the Internet at http://pubs.acs.org.

JO000146G

(41) *CS−Chem3D Pro 5.0/CS−ChemDraw Ultra 5.0 for ChemOffice 5.0*; CambridgeSoft: Cambridge, MA, 1999.
(42) Bielecki, A.; Burum, D. P. *J. Magn. Reson. A116* **1995**, 215.